

1 **Climate change and ecosystems dynamics over the last 6000 years**
2 **in the Middle Atlas, Morocco**

3
4
5 M. Nourelbait^{1,2,3}, A. Rhoujjati², A. Benkaddour², M. Carré³, F. Eynaud⁴, P. Martinez⁴, and R.
6 Cheddadi³

7
8 ¹Université Chouaib Doukkali, Laboratoire Géosciences Marines et Sciences des Sols, unité
9 associée CNRST (URAC 45), El Jadida, Morocco.

10 ²Université Cadi Ayyad, Faculté des Sciences et Techniques, unité associée CNRST (URAC
11 42), Gueliz Marrakech, Morocco.

12 ³Université Montpellier 2, Institut des Sciences de l'Evolution, UMR UM2-CNRS-IRD 5554,
13 Montpellier, France.

14 ⁴University of Bordeaux, UMR EPOC 5805, CS 50023, 33615 Pessac, Bordeaux, France.
15
16
17

18 Received: 25 July 2015 – Accepted: 28 July 2015 – Published: 1 September 2015

19
20 Correspondence to: M. Nourelbait (nourelbait.m@gmail.com)

21
22 Published by Copernicus Publications on behalf of the European Geosciences Union.

23 **Abstract**

24 The present study aims at reconstructing past climate changes and their environmental
25 impacts on plant ecosystems during the last 6000 years in the Middle Atlas, Morocco. Mean
26 January temperature (T_{jan}), annual precipitation (P_{ann}), winter (P_w) and summer (P_s)
27 precipitation and a seasonal index (SI) have all been quantified from a fossil pollen record.
28 Several bio and geo-chemical elements have also been analyzed to evaluate the links between
29 past climate, landscape and ecosystem changes.

30 Over the last 6000 years, climate has changed within a low temperature and precipitation
31 range with a trend of aridity and warming towards the present. T_{jan} has varied within a ca.
32 2°C range and P_{ann} within less than 100 mmyr^{-1} . The long-term changes reconstructed in our
33 record between 6ka cal BP and today are consistent with the aridity trend observed in the
34 Mediterranean basin. Despite the overall limited range of climate fluctuation, we observe
35 major changes in the ecosystem composition, the carbon isotopic contents of organic matter
36 ($\delta^{13}\text{C}$), the total organic carbon and nitrogen amount, and the carbon to nitrogen ratio (C/N)
37 after ca. 3750 cal BP. The main ecosystem changes correspond to a noticeable transition in
38 the conifer forest between the Atlas cedar, which expanded after 3750 cal BP, and the pine
39 forest. These vegetation changes impacted the sedimentation type and its composition in the
40 lake.

41 Between 5500 and 5000 cal BP, we observe an abrupt change in all proxies which is coherent
42 with a decrease in T_{jan} without a significant change in the overall amount of precipitation.

43 1 Introduction

44 The amplitude of climate change during the Holocene (11,700 cal BP to the present) is known
45 to be globally less extreme than during the post-glacial period (Bianchi and McCave, 1999;
46 Bond et al., 2001; Debret et al., 2007). However, several studies have shown that there were
47 climate fluctuations (Alley et al., 1997; Wanner et al., 2008) related to the internal variability
48 of the climate system, solar activity, albedo (Ruddiman, 2003; Eddy, 1982; Stuiver *et al.*,
49 1991), volcanic eruptions (Kelly and Sear, 1984; Sear et al., 1987; Bryson, 1989; Mann et al.,
50 2005), ocean circulation (Manabe and Stouffer, 1988; Dansgaard et al., 1989; Lascaratos et
51 al., 1999; Rohling et al., 2002), etc. which all have a direct impact on the terrestrial
52 ecosystems (Davis, 1963; Emmanuel *et al.*, 1985). Although climate changes were less
53 pronounced during the Holocene (Andersen et al., 2004; Mayewski et al., 2004; Witt and
54 Schumann, 2005; Frigola et al., 2007; Cheddadi and Bar-Hen, 2009) than during the last post-
55 glacial period, they have still been noticeable enough to be recorded by different proxies
56 (Dorale et al., 1992; Williams et al., 2002; Geiss et al., 2003, 2004). At the global scale, the
57 Holocene climate stability allowed a sustainable vegetation dynamics with long-term
58 ecosystems changes, plant species expansions and migrations, and an increase of species
59 diversity over all latitudes (Rohde, 1992). However, the Holocene period has also recorded
60 some abrupt and cold events such as the one at 8.2 ka cal BP (e.g. Alley and Agustsdottir,
61 2005) which recorded a depletion of about 4°C in winter temperature in the Eastern
62 Mediterranean (Weninger et al., 2009).

63 In Morocco, climate changes during the Holocene have also been quantified and they show
64 significant fluctuations (Cheddadi et al., 1998). As a matter of fact, the climate variability of
65 the Holocene is less known than that of the post-glacial (Mayewski et al., 2004) because it has
66 a lower amplitude and is less abrupt. This statement is even more acute in the Mediterranean
67 region where high resolution and chronologically well-constrained Holocene records are
68 much less numerous than in Europe or North America. The Mediterranean area is currently a
69 hotspot of biodiversity (Myers et al., 2000) and it is one of the largest regions in the world
70 that undergo long-lasting and pronounced droughts during the summer season (Roberts et al.,
71 2004; Milano et al., 2013). The southern rim of the Mediterranean region is even more arid
72 than the northern one because of the influence of the Azores high and the Saharan winds
73 which increase the impact of the drought effect during the summer season. Most of the winter
74 precipitation (Pw) originates from the trade winds which carry moisture from the
75 Mediterranean Sea (Martin, 1981). The amount of Pw has a strong impact on the persistence

76 of water bodies and on the lake levels in the Mediterranean area. Strong lake level
77 fluctuations during the Holocene were observed in Lake Van, Turkey (Lemcke and Sturm,
78 1997), Lago Dell'Accesa and Lago di Mezzano, Italy (Magny et al., 2006), lake Kinneret,
79 (Hazan et al., 2005) and the Dead Sea, Israel (Migowski et al., 2006), lake Siles, Spain
80 (Carrión, 2002), and lakes Sidi Ali and Tigalmamine in Morocco (Lamb and Van der kaars,
81 1995; Märtsche-Soulié et al., 2008).

82 The analysis of marine and continental records from the central part of the Mediterranean
83 shows that the lake levels were high between 10,300 and 4500 cal BP due to an enhanced
84 moisture availability during both summer and winter (Magny et al., 2013). After 5000 cal BP,
85 pollen data from southwestern Europe show that drought increased and led to a sustained
86 reduction of the forest cover (Roberts et al., 2001; Jalut et al., 2009; Jiménez-Moreno et al.,
87 2015). These environmental changes show that within the long-term climate trend there were
88 humid-arid episodes that are related to internal forcings of the climate system such as, in the
89 case of these westernmost Mediterranean ecosystems, the centennial changes in the North
90 Atlantic Oscillation modes (Jiménez-Moreno et al., 2015), the enhancement/weakening of the
91 trade winds, or the increase in the coastal upwelling off northwestern Africa (McGregor et al.,
92 2007).

93 Climate reconstructions from marine pollen records suggest that the Mediterranean
94 environments may react with a reduced time lag to rapid climate changes (Fletcher et al.,
95 2010). The response of the western Mediterranean ecosystems has even been synchronous
96 with the North Atlantic variability during the post-glacial period and the Holocene
97 (Combourieu-Nebout et al., 2009). Changes in the pollen assemblages of a marine record
98 from the Alboran Sea also show very synchronous fluctuations between the surrounding land
99 ecosystems changes and the sea surface temperature fluctuations (Fletcher and Sánchez Goñi,
100 2008; Combourieu-Nebout et al., 2009). Pollen records from the Middle Atlas (Reille, 1976;
101 Lamb and Van der kaars, 1995; Cheddadi et al., 2009; Rhoujjati et al., 2010; Nour el Bait et
102 al., 2014; Tabel et al., 2016) and the Rif mountains (Cheddadi et al., 2016) show that the
103 Holocene climate change had a major impact on the ecosystems composition with a clear
104 succession of different species sensitive to winter frost, strong rainfall seasonality and/or the
105 total amount of annual rainfall throughout the year.

106 The aim of the present study is to evaluate the impacts of the climate changes on the
107 ecosystems and the landscape of the Middle Atlas during the last six millennia. Our approach
108 is multidisciplinary and based on the analysis of pollen grains, elemental and isotopic
109 geochemistry and grain size from a fossil record collected in Lake Hachlaf, Middle Atlas.

110 Temperature and precipitation variables have been quantified. They show a moderate change
111 which is superimposed by an aridity trend that is combined with an increase in winter
112 temperature over the past 6000 years. We also observed some noticeable ecosystem and
113 landscape changes with one rapid and quite abrupt climate fluctuation between 5500 and 5000
114 detectable in all the proxies used.

115 2 Study area

116 The Middle Atlas Mountains, lying in northwestern Morocco, consist of two geological sets
117 called Pleated and Tabular Middle Atlas (Fig. 1a). The latter is formed by a Paleozoic
118 basement covered by a Mesozoic thick layer and Cenozoic and Quaternary volcanic flows
119 (Texier et al., 1985; Herbig, 1988; Harmand and Moukadiri, 1986). The Liasic limestone and
120 dolostone are shaped by karstic mechanisms (Martin, 1981; Baali, 1998; Hinaje and Ait
121 Brahim, 2002; Chillasse and Dakki, 2004). In this geomorphological and structural
122 composition, there exist nowadays about twenty permanent or semi-permanent natural lakes
123 (Chillasse and Dakki, 2004) among which we can find the studied site, Dayet (lake) Hachlaf
124 (33°33'20" N; 5°0'0" W; 1700m a.s.l.). This small water body is located about ten kilometers
125 North-East of Ifrane national park (Fig. 1b). Available meteorological data (HCEFLCD,
126 2004) at Dayet Hachlaf show an average annual rainfall of ca. 600 mm with Pw and Ps ca.
127 150 and ca. 70 mm, respectively. The mean January temperature is ca 4 °C with ca. 90 rainy
128 days per year, and ca. 70 frosty days among which ca. 17 with snow precipitation. The surface
129 area and depth of the lake change throughout the year reaching up to respectively 14 ha and 4
130 m during late spring. The lake is fed by rainwater, snow, surface runoff and groundwater and
131 has no river inflow.

132 The forest cover around the site (Fig. 1c) is composed of holm oak (*Q. ilex* subsp.
133 *rotundifolia*) which is evergreen and zeen oak (*Q. canariensis*) which is deciduous, and Atlas
134 cedar (*Cedrus atlantica*) with occurrences of *Pinus halepensis*. Nowadays, there are some
135 degraded populations of *Cedrus atlantica* with cultivated lands around the lake. At higher
136 altitude (1700 to 2500 m, Fig. 1c) an herbaceous/shrubby vegetation (*Artemisia herba-alba*
137 and Poaceae) dominates the landscape.

138 3 Materials and methods

139 In April 2008, a 2.5m core (33°33'2.49" N, 4°59'41.57" W) was collected using a Russian
140 corer. Each section of the core was then sub-sampled for the analysis of pollen content (30

141 samples), grain size (39 samples), organic matter (43 samples) and its isotopic composition
142 ($\delta^{13}\text{C}_{(\text{org})}$; 46 samples), and total nitrogen and carbonates (43 samples).

143 Pollen grains were extracted using a standard laboratory procedure: HCl (20 %), KOH (10
144 %), ZnCl_2 , acetolysis ($\text{CH}_3\text{CO}_2\text{O}$ and H_2SO_4), KOH (10 %), ethanol and glycerine. The
145 identification and counting of pollen grains were performed with an optical microscope (Leica
146 DM750) using a $\times 40$ magnification ($\times 63$ for accurate identifications). The pollen percentages
147 were calculated on the total sum of pollen grains originating from vascular terrestrial plants.
148 The total pollen grains counted varies between ca. 200 and 1300. Aquatic plants percentages
149 (including Cyperaceae and Juncaceae) were excluded from the total pollen sum. Cyperaceae
150 were considered as aquatic plants since there are *Juncus* and *Cyperus* genera growing around
151 the lake today.

152 The particle size analysis was carried out at the “*Laboratoire Marocain d’Agriculture*
153 (LABOMAG)” and was only performed on the sediment fraction < 2 mm. The proportions of
154 five fractions were identified as follows: coarse sand (2000–200 μm), fine sand (200–50 μm),
155 coarse silt (50–20 μm), fine silt (20–2 μm) and clay (below 2 μm).

156 Organic matter amount (OM) was estimated based on the content of the organic carbon in
157 lacustrine sediments (OC), elaborated by spectrometry (NF ISO 14235). Sediment OC was
158 oxidized in a sulfochromic environment with an excess of potassium dichromate at 135 °C.
159 Subsequently, the determination of chromate ions Cr^{3+} formed was analysed by spectrometry.
160 For total nitrogen (TN), the method used was based on the Kjeldahl mineralization (ISO
161 11464: 1994), but the catalyst used was the titanium dioxide (TiO_2). The technique consists in
162 assaying the total nitrogen content in the sediment as ammonium, nitrate, nitrite and organic
163 form.

164 Carbonates were measured by adding HCl to the bulk sediment to decompose all carbonates
165 (NF ISO 10693: Juin, 1995). The volume of the carbonic gas produced was measured using a
166 Scheibler apparatus.

167 Stable isotope ratios measurements of carbon were performed on a Thermo Fischer Flash
168 2000 Elemental Analyzer in line with a VG Isoprime Mass Spectrometer at the University of
169 Bordeaux. All samples were pretreated with 1N HCl to remove inorganic carbon. The
170 analytical precision of 0.15‰ was estimated from several calibrated laboratory standards
171 analyzed along the samples. Stable isotopic ratios were reported as: $\delta^{13}\text{C} = [({}^{13}\text{C}/{}^{12}\text{C}_{\text{sample}} /$
172 ${}^{13}\text{C}/{}^{12}\text{C}_{\text{std}}) - 1] * 1,000$, where the standard used is Vienna Pee Dee Belemnite (PDB)

173 Besides the multi-proxy analysis, four organic samples were dated. All this dates have been
174 done on bulk sediment. We used the BACON software (Blaauw and Christen, 2011) to

175 compute the age/depth model (Fig. 2). The default ^{14}C calibration curve used by BACON for
176 terrestrial northern hemisphere samples is IntCal13. The AMS ^{14}C dates were also calibrated
177 using the “CALIB 7.1” program (Stuiver and Reimer, 1986; table 1). The fossil record
178 continuously encompassed the last 6000 years.

179 Annual precipitation (P_{ann}), mean January temperature (T_{jan}) and precipitation seasonal
180 index (SI) assessment (Fig. 3) were based on pollen data as follows:

$$PSI_{(s)} = (\sum P_w - \sum P_s) / \sqrt{P_{ann}}$$

181
182 Where $PSI_{(s)}$ is the seasonal index quantified for sample s ; P_w is the sum of December,
183 January and February precipitation; P_s is the sum of June, July and August precipitation;
184 P_{ann} is the total annual precipitation.

185 The monthly mean precipitation and T_{jan} were obtained using the probability density function
186 of modern plant species (pdf-method). This method is described in Chevalier et al. (2014). In
187 order to apply it to a fossil pollen record collected in the Mediterranean area it required a
188 modern database of Mediterranean plant species distributions and their corresponding modern
189 climate variables. We used a database of plant species that have been georeferenced from
190 *Flora Europaea* (Jalas et al. 1972, 1973, 1976, 1979, 1980, 1983, 1986, 1989, 1991, 1994)
191 and Hulten and Fries (1986). Additional geographical distributions were obtained from GBIF
192 (2012) and personal field observations using GPS in Morocco. In order to use plant species
193 distributions for the pollen-based climate reconstruction we assigned pollen taxa to the most
194 probable plant species in our plant database (table 2). The modern climate variables were
195 extracted from the WORLDCLIM database (Hijmans et al., 2005) and interpolated onto the
196 species occurrences for inferring their pdfs.

197 **4 Results**

198 During the last 6000 years, the main change in the forest cover is marked by a decline of the
199 pine populations, the expansion of Atlas cedars after 3750 cal BP and the persistence of the
200 evergreen oaks. Although the latter dominate today the landscape around Lake Hachlaf, the
201 microscope identification of the fossil pollen grains that originate from deciduous or
202 evergreen plants may often be dubious and therefore, may not be reproducible by another
203 pollen analyst. We have assigned all oak pollen grains to the evergreen *Quercus ilex* in the
204 climate reconstruction since it is the species that dominates the landscape and its climate
205 envelope encompasses that of the other evergreen species (Fig. 4). All other taxa, including
206 trees, shrubs and herbs, also show some changes but within a much lower range than that of

207 the two conifer taxa, Atlas cedar and pine (Fig. 5). We have applied a constrained cluster
208 analysis to depict the main changes in the pollen fossil record. There are four main clusters
209 summarizing the main changes in the ecosystem composition around Lake Hachlaf over the
210 last 6000 years (table 3).

211 The grain size analysis revealed the presence of three fractions (Fig. 3) with the following
212 proportions: clay (22.87%), silt (60.46% with 41.9% of fine silt) and sand (16.67 %). The
213 dominant silty fraction tends to increase from the bottom to the top of the core after a brief
214 decline between ca. 5600 and 5200 cal BP. The sandy fraction follows the same pattern. Clay
215 shows an opposite trend to both the sandy and silty fractions.

216 Carbonates (CaCO_3) content is high throughout the record except around 5200 cal BP (Fig.
217 3). They are positively correlated with silt and sand. The total organic carbon (TOC) content
218 is also high and varies significantly between 4 and 27.4% (Fig. 3). The total nitrogen (TN)
219 remains low throughout the record. The carbon to nitrogen ratio (C/N) varies between 9 and
220 17.4, and the $\delta^{13}\text{C}_{\text{Org}}$ between -21 and -27‰ (Fig. 3). Two origins of the organic matter are
221 thus identified, with lake algae characterized by $\text{C/N} < 11$ and very depleted $\delta^{13}\text{C}_{\text{Org}}$ and
222 terrestrial plants characterized by $\text{C/N} > 11$ and less depleted $\delta^{13}\text{C}_{\text{Org}}$ (Fig. 6). $\delta^{13}\text{C}_{\text{Org}}$ and
223 C/N are positively correlated (Fig. 3). TOC and TN are highly correlated (0.99, Figs. 3 and 6)
224 as well.

225 In order to interpret the different bio and geo-chemical proxies within a climatic frame, a
226 pairwise correlation was performed between the three climate variables and $\delta^{13}\text{C}$, C/N, TN
227 and TOC (Fig. 7). Although there could be no causal relationship, SI and Tjan are well
228 correlated together. They are both correlated negatively with $\delta^{13}\text{C}$ and C/N and positively
229 with TN and TOC (Fig. 7).

230 **5 Discussion**

231 The Holocene climate around the Mediterranean Sea was suitable for the expansion of human
232 populations and their organization towards true civilizations (Kaniewski et al., 2012). The
233 persistence and longevity of many Mediterranean populations may be linked to the relative
234 suitability and also to an overall stability of the Holocene climate. However, climatic events
235 have been recorded within the Holocene (e.g. Rohling and Pälike, 2005) and a causal
236 relationship has been made between some abrupt climatic events and societal changes in the
237 Mediterranean (Berger and Guilaine, 2009; Kaniewski et al., 2008).

238 In the present study, we have focused on the environmental and climate changes that occurred
239 during the last 6 millennia in the northern part of the Moroccan Middle Atlas Mountains. We

240 have evaluated the vegetation dynamics using the palynological content of a fossil sequence
241 and analyzed its bio- and geo-chemical content to reconstruct the overall landscape changes.
242 The reconstructed Tjan and Pann show a relatively low amplitude of change over the last
243 6000 years (Fig. 3). *Pann* decreases progressively by ca. 100mm which is in line with the
244 aridity trend that has been observed in other fossil records (Risacher and Fritz, 1992; Brooks,
245 2006; Hastenrath, 1991; Anderson and Leng, 2004; Umbanhowar et al., 2006) and
246 particularly in the Mediterranean area (Pons and Reille, 1988; Julià et al., 2001; Burjachs et
247 al., 1997; Yll et al., 1997; Roberts et al., 2001; Valino et al., 2002, Jalut et al., 2009) and
248 northern Africa (Ritchie, 1984; Ballouche, 1986; Lamb et al., 1989). At a more regional scale,
249 reconstructed *Pann* is coherent with that obtained from Lake Tigalmamine (Cheddadi et al.,
250 1998) which shows a decreasing trend over the last ca. 5000 cal BP. The arid trend observed
251 after ca. 5ka cal BP is marked by a spread of Poaceae and a progressive replacement of pines
252 by Atlas cedars which better stand the high seasonal contrast of precipitation at the altitude of
253 Hachlaf Lake. *SI* increases from 3 to 7 times over the last 6000 years (Fig. 3). A study of
254 drought thresholds influencing the growth and photosynthesis was performed on different
255 cedar stands and species (*C. atlantica*, *C. libani*, *C. brevifolia* and *C. deodora*) of different
256 origins (Aussenac and Finkelstein, 1983). This study showed that among many conifers, cedar
257 trees may keep a sustained photosynthesis activity even when drought is very high. Thus, a
258 strong precipitation contrast between *Ps* and *Pw* (Fig. 3) may not affect the Atlas cedar overall
259 growth as long as the total amount of rainfall is sufficient (higher than 600 mm/year) and the
260 winter temperature is low enough (below 6°C) for the vegetative cycle (Aussenac et al.,
261 1981). The Mediterranean climate is known for its strong seasonal distribution of precipitation
262 throughout the year. Summers are fairly dry and most of the annual precipitation occurs
263 during the cold months (end of autumn and beginning of winter).

264 Currently, 75% of the Moroccan territory with a grassy or wooded vegetation (thus excluding
265 the desert) records between 500 and 800mm of annual rainfall with an *SI* between 5 and 8
266 (Fig. 8). The whole range of *SI* in Morocco is between -1 in areas where *Pann* is less than
267 100mm with a random distribution as for instance in the South of Morocco, and 15 in areas
268 where the annual rainfall is quite high (over 800 mm) and occurs mainly in the winter season
269 such as in the Rif mountains today (Fig. 8). *SI* is higher in mountainous areas. Nowadays, in
270 the areas surrounding Hachlaf lake (located at ca. 1600m elevation) *SI* is around 5. Such *SI*
271 has changed over the past thousand years as confirmed, at least between 6000 cal BP and
272 today, by the studied fossil archive (Fig. 3). The amplitude between *Pw* and *Ps* precipitation
273 has increased 2 to 3 times towards the present (Fig. 3). Since *Pann* has a decreasing trend, the

274 opposite increased seasonality is related to a significant reduction in the amount of rainfall
275 during the months of June, July and August (Fig. 3). This strengthening of the contrast
276 between Pw and Ps had a rather limited impact on the dominating taxa because they can
277 withstand the summer drought and the overall amount of Pw remained sufficient for their
278 persistence. However, a change in the amplitude of SI has probably favoured those species
279 best adapted to the length of the dry season, as for instance evergreen oaks rather than
280 deciduous. Pollen-based climate reconstructions from records collected in the Alboran Sea
281 (Combourieu-Nebout et al., 2009) and Italy (Magny et al., 2013; Peyron et al., 2013) suggest
282 a rather steady and low seasonal contrast between Pw and Ps (about two times) over the past
283 6000 years cal BP. Such discrepancy between the reconstructed SI from Hachlaf and the
284 marine record may potentially be related to the fact that marine records collect pollen grains
285 from a much wider geographical source area than continental (mountainous) records which
286 probably tends to smooth the local/regional changes. The reconstructed seasonality from the
287 Italian records (Magny et al., 2013; Peyron et al., 2013) is buffered by the less abrupt
288 precipitation seasonal contrast at the European temperate latitude than at the arid
289 Mediterranean one.

290 SI was lower than 5 before 3750 cal BP despite an amount of precipitation between 600 and
291 700 mm yr^{-1} (Fig. 3). During that period, water probably persisted in the lake all throughout
292 the year which allowed the presence of aquatic plants (Fig. 5) flowering during late spring and
293 summer, and algae identified in the pollen data, through the low values of $\delta^{13}\text{C}_{\text{org}}$ and the
294 C/N ratio being greater than 11 (Figs. 3 and 5). The proportion of aquatic plants cannot be
295 directly related to a high lake level and may not be used to state the lake level changes but
296 only the presence of water in the site. The $\delta^{13}\text{C}_{\text{org}}$ and C/N (Fig. 6) provide information
297 concerning the origin of the organic matter (*in situ* production versus input from the
298 catchment area) but not on the lake level changes. Thus, high $\delta^{13}\text{C}_{\text{org}}$ and C/N ratios (Fig. 3)
299 with low presence of aquatic plants (Fig. 5) may not be inconsistent in cases where there is a
300 low terrestrial input (low Sand/Silt, Fig. 3) during a period when the lake level is high.

301 The relationship between $\delta^{13}\text{C}_{\text{org}}$ and the C/N ratio indicates the occurrence of two main
302 types of organic matter mainly originating from a C3 metabolism. Lacustrine algae can be
303 considered as dominantly autochthonous; in the lower part of the record, the organic matter,
304 with higher C/N ratios and less depleted $\delta^{13}\text{C}_{\text{org}}$ corresponds to a terrestrial input. Indeed,
305 Fresh organic matter from lake algae is known to be protein-rich and cellulose-poor with
306 molar C/N values commonly between 4 and 10, whereas vascular land plants, are protein-poor
307 and cellulose-rich, creating organic matter usually with C/N ratios of 20 and greater (Meyers,

308 1994, 2003). However, a C/N ratio > 11 may correspond to a mixture of both local and
309 terrestrial organic matter (Fig. 6).

310 After 3750 cal BP, Atlas cedars noticeably spread around the site while the pine populations
311 strongly regress. A series of fossil pollen records in the Middle Atlas show that Atlas cedar
312 populations expanded after ca. 6 ka cal BP. The sustained expansion of Atlas cedar after ca.
313 3750 cal BP around Hachlaf Lake expresses its late occurrence at higher altitude. Around lake
314 Tigalmamine (Lamb et al., 1995), the Ras El Ma marsh (Nour El Bait et al., 2014) and the Ait
315 Ichou marsh (Tabel et al., 2016) which are all located at about 100 to 200 meters altitude
316 below Hachlaf lake (ca. 1700m asl), Atlas cedar occurs much earlier. The expansion of Atlas
317 cedar around the lake is probably related to both an upslope spread and a south-north
318 migration.

319 During this ecosystem transition we observe a major change in both Pann and Tjan. The
320 increase of SI after 3750 cal BP is due to a combined increase of Pw and decrease of Ps (Fig.
321 3). The expansion of cedar forests in the studied area may be related to their better adaptation
322 to strong SI than pines at higher altitude.

323 Competition is another parameter that might be worth considering. After 3750 cal BP, the
324 C/N ratio is below 11 and the $\delta^{13}\text{C}$ remains below -26‰ which suggest the important primary
325 productivity of the lake associated with low input of land plant derived organic matter. Atlas
326 cedar forests have a more important growth in both height and diameter than pines which
327 leads to a higher biomass production. This is linked to the genetic model of growth that is
328 very distinct between the two taxa (Kaushal et al., 1989). Thus, the expansion of Atlas cedar
329 population around the site may explain the high input of OM into the lake.

330 Over the last six millennia, superimposed to the overall climate trend, we observe one
331 relatively abrupt event between 5500 and 5000 cal BP during which Tjan declined by about
332 2°C compared to its average over 6000 years. A climatic transition between 6 and 5 ka cal BP
333 at the end of the Holocene thermal maximum has been globally identified (Steig, 1999;
334 Mayewski et al., 2004; Wanner et al., 2008; Brooks, 2012). This transition has been recorded
335 by a wide range of climate proxies (e.g. Kaufman et al., 2004; Jansen et al., 2009; Seppä et
336 al., 2009; Bartlein et al., 2011) and has been related to different biosphere feedbacks and
337 potentially to a decay of the remaining Laurentide ice sheet (Renssen et al., 2009). All proxies
338 from the Hachlaf sequence as well as the reconstructed climate variables have recorded
339 marked changes during that period of time. SI has the lowest value of the record and a
340 succession of abrupt changes are recorded in the C/N ratio, the grain size fractions, the $\delta^{13}\text{C}$,
341 TN, TOC and CaCO_3 (Fig. 3). Carbonates, considered as a “paleo-thermometer” (Meyers,

342 1994, 2003), also decrease abruptly around 5200 cal BP (Fig. 3). The latter may be linked to a
343 low evaporation of the lake which may have been favored by low winter temperature around
344 5200 cal BP. The fine grain size sediment also increased as a consequence of low seasonal
345 precipitation contrast and/or a continuous sediment input to the lake. Such sustained input of
346 clay and decreasing carbonate content suggest a higher lake level between 5500 and 5000 cal
347 BP (Fig. 3). Thus, the Tjan and SI decrease may have contributed to the higher lake level or at
348 least to the presence of water throughout the year (Fig. 3). At the same time, the sand to silt
349 ratio is very low which confirms a low energy during the sedimentation process. The major
350 change in the ecosystem composition around the lake is the rapid collapse of the pine forest
351 which has inevitably released an important amount of terrestrial carbon (biomass) into the
352 lake (positive peaks in $\delta^{13}\text{C}$ and C/N, Fig. 3).

353 **6 Conclusions**

354 This study marks a new contribution to the knowledge of past climates and environmental
355 history in North Africa mountainous areas. The range of climate change in the Middle Atlas,
356 Morocco, was rather minor between 6000 cal BP and the present. Annual precipitation and
357 January mean temperature have respectively varied within a range of 100 mm and 2 to 3°C.
358 However, they both show a trend towards a more arid and warmer climate as well as a higher
359 rainfall seasonality. Pann became as contrasted as today after 3750 cal BP. The aridity trend
360 observed in Hachlaf over the last 6000 years is consistent with other climate reconstructions
361 available from other Mediterranean fossil records. Besides these overall climatic trends, we
362 also observe an abrupt cold event between 5500 and 5000 cal BP which is well marked in all
363 environmental proxies from our studied fossil record. The $\delta^{13}\text{C}$ and C/N ratios, which are well
364 correlated together, suggest an increase in the organic matter input from the catchment area.
365 Concomitantly, the pollen record indicates a decline of the pine forest which may have
366 contributed to the organic matter input into the lake too. The marked change in both the
367 carbonates content and clay composition of the record were probably related to a perennial
368 presence of water throughout the year. Synchronously, seasonality index and January mean
369 temperature were the lowest of the record which has contributed to a reduction of the
370 evaporation.

371 The increase in rainfall seasonality has probably favored the expansion of Atlas cedars around
372 the studied site at the expense of the pine forest.

373

374 ***Acknowledgements.*** This work was supported by the Volubilis Program (Programme mixte
375 Interuniversitaire Franco-marocain, MA/11/251), 2011, by CNRS-CNRST Convention, 2009
376 (ScVie07/09) and the French national program EC2CO-Biohefect, “Variabilité
377 paléoclimatique et impact sur les forêts de conifères au Maroc depuis la période glaciaire”.
378 MN received a postdoc grant from the EU Framework Programme Erasmus Mundus EU
379 METALIC II (2013-2442 / 001-001 – EMA2) for completing this study at ISEM. We thank
380 Claire Grandchamps for her revision of the English version of the manuscript. This is an
381 ISEM contribution n° 2016-020.

382 **References**

- 383 Alley, R. B., Mayewski, P. A., Sowers, T., Stuiver, M., Taylor, K. C., and Clark, P. U.:
384 Holocene climatic instability: a prominent, widespread event 8200 yr ago, *Geology*, 25, 483–
385 486, 1997.
- 386 Alley, R.B., Agustsdottir, A.M.: The 8k event: cause and consequences of a major Holocene
387 abrupt climate change, *Quat. Sci. Rev.*, 24, 1123–1149, 2005.
- 388 Andersen, C., Koç, N., Jennings, A., and Andrews, J. T.: Non uniform response of the major
389 surface currents in the Nordic Sea to insolation forcing: implications for the Holocene climate
390 variability, *Paleoceanography*, 19, PA2003, doi:10.1029/2002PA000873, 2004.
- 391 Anderson, N. J. and Leng, M. J.: Increased aridity during the early Holocene in West
392 Greenland inferred from stable isotopes in laminated-lake sediments, *Quat. Sci. Rev.*, 23,
393 841–849, 2004.
- 394 Aussenac, G. and Finkelstein, D.: Influence de la sécheresse sur la croissance et la
395 photosynthèse du cèdre, *Ann. Sci. for.*, 40, 67–77, 1983.
- 396 Aussenac, G., Granier, A., and Gross, P.: Etude de la croissance en hauteur du Cèdre (*Cedrus*
397 *atlantica* Manetti) Utilisation d'un appareillage de mesure automatique, *Ann. Sci. for.*, 38,
398 301–316, 1981.
- 399 Baali, A.: Genèse et évolution au Plio-Quaternaire de deux bassins intramontagneux en
400 domaine carbonaté méditerranéen. Les bassins versants des dayets Afourgagh et Agoulmam
401 (Moyen Atlas, Maroc), PhD thesis, University of Rabat, 326 pp., 1998.
- 402 Ballouche, A. : Paléoenvironnements de l'homme fossile holocène au Maroc. Apports de la
403 palynologie, PhD thesis, University of bordeaux, 134 pp., 1986.
- 404 Bartlein, P.J., Harrison, S.P., Brewer, S., Connor, S., Davis, B.A.S., Gajewski, K., Guiot, J.,
405 Harrison-Prentice, T.I., Henderson, A., Peyron, O., Prentice, I.C., Scholze, M., Seppä, H.,
406 Shuman, B., Sugita, S., Thompson, R.S., Vial, a. E., Williams, J., Wu, H.: Pollen-based
407 continental climate reconstructions at 6 and 21 ka: a global synthesis. *Clim. Dyn.*, 37, 775–
408 802, 2011.

409 Berger, J. F. and Guilaine, J.: The 8200 cal BP abrupt environmental change and the
410 Neolithic- transition: a Mediterranean perspective, *Quat. Int.*, 200, 31–49, 2009.

411 Bianchi, G. G. and McCave, N.: Holocene periodicity in North Atlantic climate and deep-
412 ocean flow south of Iceland, *Nature*, 397, 515–517, 1999.

413 Blaauw, M. and Christen, J.A.: Flexible Paleoclimate Age-Depth Models Using an
414 Autoregressive Gamma Process, *Bayesian Analysis*, 6, 457–474, 2011.

415 Bond, G., Kromer, B., Beer, J., Muscheler, R., Evans, M., Showers, W., Hoffmann, S., Lotti-
416 Bond, R., Hajdas, I., and Bonani, G.: Persistent solar influence on North Atlantic climate
417 during the Holocene, *Science*, 294, 2130–2136, 2001.

418 Brooks, N.: Beyond collapse: climate change and causality during the Middle Holocene
419 Climatic Transition, 6400–5000 years before present, *Geogr. Tidsskr. Geogr.*, 112, 93–104,
420 doi:10.1080/00167223.2012.741881, 2012.

421 Brooks, N.: Cultural responses to aridity in the middle Holocene and increased social
422 complexity, *Quat. Int.*, 151, 29–49, 2006.

423 Bryson, R.A.: Late Quaternary volcanic modulation of Milankovitch climate forcing. *Theor.*
424 *Appl. Climatol.*, 39, 115–125, 1989.

425 Burjachs, F., Giralt, S., Roca, J.R., Seret, G., and Julia, R.: Palinologia holocenica y
426 desertizacion en el Mediterraneo occidental. *El Paisaje Mediterraneo a Traves del Espacio y*
427 *del Tiempo. Implicaciones en la Desertificacion* (eds J.J. Ibanez, B.L. Valero and C.
428 Machado), 379–394. Geoforma Editores, Logrono, Spain, 1997.

429 Carrión, J. S.: Patterns and processes of Late Quaternary environmental change in a montane
430 region of Southwestern Europe, *Quat. Sci. Rev.*, 21, 2130–2136, 2002.

431 Cheddadi, R., Lamb, H.F., Guiot, J., and van der Kaars, S.: Holocene climatic change in
432 Morocco: a quantitative reconstruction from pollen data. 14, 883–890, 1998.

433 Cheddadi, R. and Bar-Hen, A.: Spatial gradient of temperature and potential vegetation
434 feedback across Europe during the late Quaternary, *Clim. Din.*, 32, 371–379, 2009.

435 Cheddadi, R., Bouaissa, O., Rhoujjati, A. and Dezileau, L.: Holocene Environmental changes
436 in the Rif Mountains, Morocco. *Quat.*, 27, 15–25, 2016.

437 Cheddadi, R., Fady, B., François, L., Hajar, L., Suc, J. P., Huang, K., Demarteau, M.,
438 Vendramin, G. G., and Ortu, E.: Putative glacial refugia of *Cedrus atlantica* from Quaternary
439 pollen records and modern genetic diversity, *J. Biogeogr.*, 36, 1361–1371, 2009.

440 Chevalier, M., Cheddadi, R. and Chase, B. M.: CREST (Climate REconstruction SofTware):
441 a probability density function (PDF)-based quantitative climate reconstruction method, *Clim.*
442 *Past*, 10, 2081–2098, doi:10.5194/cp-10-2081-2014, 2014.

443 Chillasse, L. and Dakki, M.: Potentialités et statuts de conservation des zones humides du
444 Moyen-Atlas (Maroc), avec référence aux influences de la sécheresse, *Sécheresse*, 15, 337–
445 45, 2004.

446 Combourieu-Nebout, N., Peyron, O., Dormoy, I., Desprat, S., Beaudouin, C., Kotthoff, U.,
447 and Marret, F.: Rapid climatic variability in the west Mediterranean during the last 25 000
448 years from high resolution pollen data, *Clim. Past*, 5, 503–521, doi:10.5194/cp-5-503-2009,
449 2009.

450 Dansgaard, W., White, J.W.C., and Johnsen, S.J.: The abrupt termination of the Younger
451 Dryas climatic event, *Nature*, 339, 532–534, 1989.

452 Davis, M.B.: On the theory of pollen analysis. *Am. J. Sci.*, 261, 899–912, 1963.

453 Debret, M., Bout-Roumazeilles, V., Grousset, F., Desmet, M., McManus, J. F., Massei, N.,
454 Sebag, D., Petit, J.-R., Copard, Y., and Trentesaux, A.: The origin of the 1500-year climate
455 cycles in Holocene North-Atlantic records, *Clim. Past*, 3, 569–575, doi:10.5194/cp-3-569-
456 2007, 2007.

457 Dorale, J. A., Gonzalez, L. A., Reagan, M. K., Pickett, D. A., Murrell, M. T., and Baker, R.
458 G.: A high resolution record of Holocene climate change in speleothem calcite from Cold
459 Water Cave, northeast Iowa, *Science*, 258, 1626–1630, 1992.

460 Eddy, J.A.: The solar constant and surface temperature. *AIP Conf. Proc*, La Jolla, CA, USA,
461 9-11 March 1981, 82, 247, 1982.

462 Emmanuel, W.R., Shugart, H.H. and Stevenson, M.P.: Climate change and the broad-scale
463 distribution of terrestrial ecosystem complexes. *Clim. Chang.*, 7, 29–43, 1985.

464 Fletcher, W., J., Sánchez Goñi, M., F., Allen, J. R. M., Cheddadi, R., Combourieu-Nebout,
465 N., Huntley, B., Lawson, I., Londeix, L., Magri, D., Margari, V., Müller, U. C., Naughton, F.,
466 Novenko, E., Roucoux, K. and Tzedakis, P.C.: Millennial-scale variability during the last
467 glacial in vegetation records from Europe. *Quat. Sci. Rev.*, 29, 2839–2864, 2010.

468 Fletcher, W.J. and Sánchez Goñi, M.F.: Orbital- and sub-orbital-scale climate impacts on
469 vegetation of the western Mediterranean basin over the last 48,000 yr, *Quat. Res.*, 70, 451–
470 464, 2008.

471 Frigola, J., Moreno, A., Cacho, I., Canals, M., Sierro, F. J., Flores, J. A., Grimalt, O., Hodell,
472 D., and Curtis, J. H.: Holocene climate variability in the western Mediterranean region from a
473 deepwater sediment record, *Paleoceanography*, 22, PA2209, doi:10.1029/2006PA001307,
474 2007.

475 GBIF: Recommended practices for citation of the data published through the GBIF Network.
476 Version 1.0 (Authored by Vishwas Chavan), Copenhagen: Global Biodiversity Information
477 Facility, 12, ISBN: 87-92020-36-4.
478 http://links.gbif.org/gbif_best_practice_data_citation_en_v, 2012.

479 Geiss, C. E., Banerjee, S. K., Camill, P., and Umbanhowar, J. C. E.: Sediment-magnetic
480 signature of land-use and drought as recorded in lake sediment from south-central Minnesota,
481 USA, *Quat. Res.*, 62, 117–125, 2004.

482 Geiss, C. E., Umbanhowar, C. E. J., Camill, P., and Banerjee, S. K.: Sediment magnetic
483 properties reveal Holocene climate change along the Minnesota prairie-forest ecotone,
484 *Paleolimnol.*, 30, 151–166, 2003.

485 Harmand, C. and Moukadiri, A.: Synchronisme entre tectonique compressive et volcanisme
486 alcalin: exemple de la province quaternaire du Moyen Atlas (Maroc), *B. Soc. Geol. Fr.*, 8,
487 595–603, 1986.

488 Hastenrath, S.: *Climate Dynamics of the Tropics*, Kluwer Academic Publishers, 1383-8601,
489 Springer Netherlands, 463–488 pp., 1991.

490 Hazan, N., Stein, M., Agnon, A., Marco, S., Nadel, D., Negendank, J. F. W., Schwab, M., and
491 Neev, D.: The late Pleistocene–Holocene limnological history of Lake Kinneret (Sea of
492 Galilee), Israel, *Quat. Res.*, 63, 60–77, 2005.

493 HCEFLCD : Haut-Commissariat aux Eaux et Forêts et Lutte Contre la Désertification. Bilan
494 annuel, Santé des Forêts au Maroc. Etudes d'aménagement concerté des forêts et des parcours
495 collectifs de la province d'Ifrane. Composante III : études forestières. Rapports 9 et 10, 2004.

496 Herbig, H. G.: Synsedimentary tectonics in the Northern Middle Atlas (Morocco) during the
497 Late Cretaceous and Tertiary, in: *The Atlas System of Morocco*, edited by: Jacobshagen, V.,
498 Springer-Verlag, Berlin, 321–337, 1988.

499 Hijmans, R. J., Cameron, S. E., Parra, J. L., Jones, P. G., and Jarvis, A.: Very high resolution
500 interpolated climate surfaces for global land areas, *Int. J. Climatol.*, 25, 1965–1978, 2005.

501 Hinaje, S. and Ait Brahim, L.: Les Bassins Lacustres du Moyen Atlas (Maroc): un exemple
502 d'Activité Tectonique Polyphasée Associée à des Structures d'Effondrement, *Com. Instituto*
503 *Geológico e Mineiro*, 89, 283–294, 2002.

504 Hulten, E. and Fries, M.: *Atlas of North European vascular plants: north of the Tropic of*
505 *Cancer I-III*. Koeltz Scientific Books, Königstein, DE, 1986.

506 ISO 11464: 1994. Qualité du sol-Prétraitement des échantillons pour analyses physico-
507 chimiques. Norme révisée par ISO 11464 : 2006, 11, 2006.

508 Jalas, J. and Suominen, J.: (eds) *Atlas florae Europaeae*. Distribution of vascular plants in
509 Europe. The Committee for Mapping the Flora of Europe and Societas Biologica Fennica
510 Vanamo, Helsinki, vols 1–10, 1972, 1973, 1976, 1979, 1980, 1983, 1986, 1989, 1991, 1994.

511 Jalut, G., Dedoubat, J. J., Fontugne, M. and Otto, T. : Holocene circum-Mediterranean
512 vegetation changes: Climate forcing and human impact. *Quat. Int.*, 200, 4–18, 2009.

513 Jansen, E., Andersson, C., Moros, M., Nisancioglu, K. H., Nyland, B. F. and Telford, R. J.:
514 The Early to Mid-Holocene Thermal Optimum in the North Atlantic, in *Natural Climate*
515 *Variability and Global Warming: A Holocene Perspective* (eds R. W. Battarbee and H. A.
516 Binney), Wiley Blackwell, Oxford, UK. doi: 10.1002/9781444300932.ch5, 2009.

517 Jiménez-Moreno, G., Rodríguez-Ramírez, A., Pérez-Asensio, J. N., Carrión, J. S., López-
518 Sáez, J. A., Villarías-Robles, J. J. R., Celestino-Pérez, S., Cerrillo-Cuenca, E., León, A., and
519 Contreras, C.: Impact of late-Holocene aridification trend, climate variability and geodynamic
520 control on the environment from a coastal area in SW Spain, *Holocene*, 25, 607–627,
521 doi:10.1177/0959683614565955, 2015.

522 Julià, R., Riera, S., and Wansard, G.: Advances in Mediterranean lacustrine studies and future
523 prospects: the Southern European group of ELDP project (1999– 2001) contribution, *Terra*
524 *Nostra*, 3, 43–51, 2001.

525 Kaniewski, D., Paulissen, E., Van Campo, E., Al-Maqdissi, M., Bretschneider, J., and Van
526 Lerberghe, K.: Middle East coastal ecosystem response to middle-to-late Holocene abrupt
527 climate changes, *Proc. Natl. Acad. Sci. U.S.A.*, 16, 13941–13946,
528 doi:10.1073/pnas.0803533105, 2008.

529 Kaniewski, D., Van Campo, E., and Weiss, H.: Drought is a recurring challenge in the Middle
530 East, *Proc. Natl. Acad. Sci. U.S.A.*, 109, 3862–3867, 2012.

531 Kaufman, D. S., Ager, T. A., Anderson, N. J., Anderson, P. M., Andrews, J. T., Bartlein, P. J.,
532 Brubaker, L. B., Coats, L.L., Cwynar, L. C., Duvall, M. L., Dyke, a. S., Edwards, M.E.,
533 Eisner, W.R., Gajewski, K., Geirsdóttir, a., Hu, F.S., Jennings, A.E., Kaplan, M.R., Kerwin,
534 M.W., Lozhkin, a. V., MacDonald, G.M., Miller, G.H., Mock, C.J., Oswald, W.W., Otto-
535 Bliesner, B.L., Porinchu, D.F., Rühland, K., Smol, J.P., Steig, E.J., and Wolfe, B.B.:
536 Holocene thermal maximum in the western Arctic (0–180°W), *Quat. Sci. Rev.*, 23, 529–560,
537 doi:10.1016/j.quascirev.2003.09.007, 2004.

538 Kaushal, P., Guehl, J. M., and Aussenac, G.: Differential growth response to atmospheric
539 carbon dioxide enrichment in seedlings of *Cedrus atlantica* and *Pinus nigra* ssp. *Laricio* var.
540 *Corsicana*, *Can. J. For. Res.*, 19, 1351–1358, 1989.

541 Kelly, P.M. and Sear, C.B.: Climatic impact of explosive volcanic eruptions. *Nature*, 311,
542 740–743, 1984.

543 Lamb, C.J., Lawton, M.A., Dron, M., and Dixont, R.A.: Signals and Transduction
544 Mechanisms for Activation of Plant Defenses against Microbial Attack, *Cell*, 56, 215–224,
545 1989.

546 Lamb, H. F. and Van der Kaars, S.: Vegetational response to Holocene climatic change:
547 pollen and palaeolimnological data from the Middle Atlas, *Holocene*, 5, 400–408, 1995.

548 Lamb, H.F., Gasse, F., Benkaddour, A., El Hamouti, N., van der Kaars, S., Perkins, W.
549 T., Pearce, N. J., and Roberts, C. N.: Relation between century-scale Holocene arid intervals
550 in tropical and temperate zones, *Nature*, 373, 134–137, doi:10.1038/373134a0, 1995.

551 Lascaratos, A., Roether, W., Nittis, K., and Klein, B.: Recent changes in deep water formation
552 and spreading in the eastern Mediterranean Sea: a review, *Prog. Oceanography*, 44, 5–36,
553 1999.

554 Lecompte, M.: La végétation du moyen atlas central. Esquisse phyto-écologique et carte des
555 séries de végétation au 1/200 000, *Rev. geogr. Maroc.*, 16, 1–31, 1969.

556 Lemcke, G. and Sturm, M.: ^{18}O and trace element measurements as proxy for the
557 reconstruction of climate changes at Lake Van (Turkey): preliminary results, in: Third
558 Millenium BC Climate Change and Old World Collapse (Proceedings of the NATO
559 Advanced Research Workshop on Third Millenium BC Abrupt Climate Change and Old
560 World Social Collapse, held at Kemer, Turkey, 19–24 September 1994), edited by: Nüzhet
561 Dalfes, H., Kukla, G., and Weiss, H., Springer, Berlin, Heidelberg, New York, 653–678,
562 1997.

563 Magny, M., Combourieu-Nebout, N., de Beaulieu, J. L., Bout-Roumazeilles, V., Colombaroli,
564 D., Desprat, S., Francke, A., Joannin, S., Peyron, O., Revel, M., Sadori, L., Siani, G., Sicre,
565 M. A., Samartin, S., Simonneau, A., Tinner, W., Vanni`ere, B., Wagner, B., Zanchetta, G.,
566 Anselmetti, F., Brugiapaglia, E., Chapron, E., Debret, M., Desmet, M., Didier, J., Essallami,
567 L., Galop, D., Gilli, A., Haas, J. N., Kallel, N., Millet, L., Stock, A., Turon, J. L., and Wirth,
568 S.: North–south palaeohydrological contrasts in the central Mediterranean during the
569 Holocene: tentative synthesis and working hypotheses, *Clim. Past.*, 9, 1901–1967,
570 doi:10.5194/cpd-9-1901-2013, 2013.

571 Magny, M., De Beaulieu, J. L., Drescher-Schneider, R., Vanniere, B., Waltersimonnet, A. V.,
572 Millet, L., Bossuet, G., and Peyron, O.: Climatic oscillations in central Italy during the Last
573 Glacial–Holocene transition: the record from Lake Accesa, *J. Quat. Sci.*, 21, 311–320, 2006.

574 Manabe, S. and Stouffer, R. J.: Two stable equilibria of a coupled ocean-atmosphere model. *J.*
575 *Clim.*, 1, 841–866, 1988.

576 Mann, M. E., Cane, M. A., Zebiak, S. E. and Clement, A.: Volcanic and solar forcing of the
577 tropical Pacific over the past 1000 years. *J. Clim.*, 18, 447–456, 2005.

578 Märsche-Soulié, I., Benkaddour, A., Elkhiaï, N., Gemayel, P., and Ramdani, M.:
579 Charophytes, indicateurs de paléo-bathymétrie du lac Tigalmamine (Moyen Atlas, Maroc),
580 *Geobios*, 41, 435–444, 2008.

581 Martin, J.: Carte géomorphologique du Moyen Atlas central au 1/100.000, Notes et Mém.
582 *Serv. géol. Maroc*, 258 bis, 445 pp., 1973.

583 Martin, J.: Le Moyen Atlas central étude géomorphologique, Notes et Mémoires du service
584 *Géologique N° 258 bis Rabat Maroc*, 447 pp, 1981.

585 Mayewski, P. A., Rohling, E., Stager, C., Karlén, K., Maasch, K., Meeker, L. D., Meyerson,
586 E., Gasse, F., Van krevelde, S., Holmgren, K., Lee-thorp, J., Rosqvist, G., Rack, F.,
587 Staubwasser, M., Schneider, R., and Steig, E. J.: Holocene climate variability, *Quat. Res.*, 62,
588 243–255, 2004.

589 McGregor, H. V, Dima, M., Fischer, H. W., and Mulitza, S.: Rapid 20th-century increase in
590 coastal upwelling off northwest Africa. *Science*, 315, 637–9, 2007.

591 Meyers, P. A.: Preservation of elemental and isotopic source identification of sedimentary
592 organic matter, *Chem. Geol.*, 144, 289–302, 1994.

593 Meyers, P. A.: Applications of organic geochemistry to paleolimnological reconstructions: a
594 summary of examples from the Laurentian Great Lakes, *Org. Geochem.*, 34, 261–289, 2003.

595 Meyers, P. A.: Preservation of elemental and isotopic source identification of sedimentary
596 organic matter, *Chem. Geol.*, 144, 289–302, 1994.

597 Migowski, C., Stein, M., Prasad, S., Negendank, J. F. W., and Agnonc, A.: Holocene climate
598 variability and cultural evolution in the Near East from the Dead Sea sedimentary record,
599 *Quat. Res.*, 66, 421–431, 2006.

600 Milano, M., Ruelland, D., Fernandez, S., Dezetter, A., Fabre, J. Servat, E., Fritsch, J. M.,
601 Ardoïn-Bardin, S., and Thivet, G.: Current state of Mediterranean water resources and future
602 trends under global changes, *Hydrolog. Sci. J.*, 58, 498–518, doi:
603 10.1080/02626667.2013.774458, 2013.

604 Myers, N., Mittermeier, R. A., Mittermeier, C. G., da Fonseca, G. A. B., and Kent, J.:
605 Biodiversity hotspots for conservation priorities, *Nature*, 403, 853–858, 2000.

606 NF ISO 10693: Juin, 1995. Qualité du sol-Détermination de la teneur en carbonate - Méthode
607 volumétrique, 7, 1995.

608 NF ISO 14235. Qualité du sol-Dosage du carbone organique par oxydation sulfochimique,
609 11, 1998.

610 Nour El Bait, M., Rhoujjati, A., Eynaud, F., Benkaddour, A., Dezileau, L., Wainer, K.,
611 Goslar, T., Khater, C., Tabel, J., and Cheddadi, R.: An 18,000 year pollen and sedimentary
612 record from the cedar forests of the Middle Atlas, Morocco, *J. Quat. Sci.*, 29, 423–432, 2014.

613 Peyron, O., Magny, M., Goring, S., Joannin, S., de Beaulieu, J.-L., Brugiapaglia, E., Sadori,
614 L., Garfi, G., Kouli, K., Ioakim, C., and Combourieu-Nebout, N.: Contrasting patterns of
615 climatic changes during the Holocene across the Italian Peninsula reconstructed from pollen
616 data. *Clim. Past*, 9, 1233-1252, doi:10.5194/cp-9-1233-2013, 2013.

617 Pons, A. and Reille, M.: The holocene- and upper pleistocene pollen record from Padul
618 (Granada, Spain): A new study, *Palaeogeogr. Palaeoclimatol. Palaeoecol.*, 66, 255–249–263,
619 1988

620 Reille, M.: Analyse pollinique de sédiments postglaciaires dans le Moyen Atlas et le Haut
621 Atlas marocains: premiers résultats, *Ecol. Mediterr.*, 2, 153–170, 1976.

622 Renssen, H., Seppä, H., Heiri, O., Roche, D.M., Goosse, H., and Fichefet, T.: The spatial and
623 temporal complexity of the Holocene thermal maximum. *Nat. Geosci.*, 2, 411–414, 2009.

624 Rhoujjati, A., Ortu, E., Baali, A., Taïeb, M., and Cheddadi, R.: Environmental changes over
625 the past 29,000 years in the Middle Atlas (Morocco): a record from Lake Ifrah, *J. Arid
626 Environ.*, 74, 737–745, 2010.

627 Risacher, F. and Fritz, B.: Mise en évidence d'une phase climatique holocène extrêmement
628 aride dans l'Altiplano central, par la présence de la polyhalite dans le salar de Uyuni
629 (Bolivie), *Paleoclimatology, CR. Acad. Sci. Paris*, 314, 1371–1377, 1992.

630 Ritchie, M. : Analyses polliniques de sédiments holocènes supérieurs des Hauts-Plateaux du
631 Maghreb oriental, *Pollen Spores, Paris*, 16, 489–496, 1984.

632 Roberts, N., Reed, J. M., Leng, M. J., Kuzucuoglu, C., Fontugne, M., Bertaux, J., Woldring,
633 H., Bottema, S., Black S., Hunt, E., and Karabiyikoglu, M.: The tempo of Holocene climatic
634 change in the eastern Mediterranean region: new high-resolution crater-lake sediment data
635 from central Turkey, *Holocene*, 11, 721–736, 2001.

636 Roberts, N., Stevenson, T., Davis, B., Cheddadi, R., Brewer, S., and Rosen, A.: Holocene
637 climate, environment and cultural change in the circum Mediterranean region, in: *Past*
638 *Climate Variability through Europe and Africa*, edited by: Battarbee, R. W., Gasse, F., and
639 Stickley, C. E., Kluwer Academic Press, Dordrecht, 343–362, 2004.

640 Rohde, K.: Latitudinal gradients in species diversity: The search for the primary cause, *Oikos*,
641 65, 514–527, 1992.

642 Rohling, E. J. and Pälike, H.: Centennial-scale climate cooling with a sudden cold event
643 around 8,200 years ago, *Nature*, 434, 975–979, doi:10.1038, 2005.

644 Rohling, E., Mayewski, P., Abu-Zied, R., Casford, J., and Hayes, A.: Holocene atmosphere-
645 ocean interactions: records from Greenland and the Aegean Sea, *Clim. Dyn.*, 18, 587–593,
646 2002.

647 Ruddiman, W. F.: Orbital insolation, ice volume, and greenhouse gases, *Quat. Sci. Rev.*, 22,
648 1597–1629, 2003.

649 Sear, C.B., Kelly, P.M., Jones, P.D. and Goodess, C. M.: Global surface-temperature
650 responses to major volcanic eruptions, *Nature*, 330, 365–367, 1987.

651 Seppä, H., Bjune, A.E., Telford, R.J., Birks, H.J.B., and Veski, S.: Last nine-thousand years
652 of temperature variability in Northern Europe, *Clim. Past.*, 5, 523–535, 2009.

653 Steig, E.J.: Mid-Holocene climate change. *Science*, 286, 6–8, 1999.

654 Stuiver, M. and Reimer, P. J.: Extended ^{14}C data base and revised calib 3.0 ^{14}C age calibration
655 program, *Radiocarbon*, 35, 215–230, 1986.

656 Stuiver, M., Braziunas, T. F., Becker, B. and Kromer, B.: Climatic, solar, oceanic and
657 geomagnetic influences on late-glacial and Holocene atmosphere $^{14}\text{C}/^{12}\text{C}$ change, *Quat. Res.*,
658 35, 1–24, 1991.

659 Tabel, J., Khater, K., Rhoujjati, A., Dezileau, L., Bouimetarhan, I., Carré, C., Vidal., L.,
660 Benkaddour, A., Nour El Bait, M., and Cheddadi, R. : Environmental changes over the past
661 25,000 years in the southern Middle Atlas, Morocco, *J. Quat. Sci.*, in press, DOI:
662 10.1002/jqs.2841, 2016.

663 Texier, J. P., Raynal, J. P., and Lefevre, D.: Nouvelles positions pour un cadre chronologiques
664 raisonné du Quaternaire marocain, *CR. Acad. Sc. Paris*, 301, 183–188, 1985.

665 Umbanhowar, C. E. J., Camill, P., Geiss, C. E., and Teed, R.: Asymmetric vegetation
666 responses to mid-Holocene aridity at the prairie-forest ecotone in south-central Minnesota,
667 *Quat. Res.*, 66, 53–66, 2006.

668 Valino, M.D., Rodríguez, A.V., Zapata, M.B.R., Garcia, M.J.G., and Gutiérrez, I.B.:
669 Climatic changes since the Late-glacial/Holocene transition in La Mancha Plain (South-
670 central Iberian Peninsula, Spain) and their incidence on Las Tablas de Daimiel marshlands,
671 *Quat. Int.*, 73–84, 2002.

672 Wanner, H., Beer, J., Bütikofer, J., Crowley, T. J., Cubasch, U., Flückiger, J., Goosse, H.,
673 Grosjean, M., Joos, F., Kaplan, J. O., Küttel, M., Müller, S. A., Prentice, I. C., Solomina, O.,
674 Stocker, T. F., Tarasov, P., Wagner, M., and Widmann, M.: Mid- to Late Holocene climate
675 change: an overview, *Quat. Sci. Rev.*, 27, 1791–1828, 2008.

676 Weninger B., Clare L., Rohling E. J., Bar-Yosef O., Böhner U., Budja M., Bundschuh M.,
677 Feurdean A., Gebel H.-G., Jöris O., Linstädter J., Mayewski P., Mühlenbruch T., Reingruber
678 A., Rollefson G., Schyle D., Thissen L., Todorova H., and Zielhofer C.: The Impact of Rapid
679 Climate Change on prehistoric societies during the Holocene in the Eastern Mediterranean,
680 *Documenta Praehistorica*, 36, 7–59, 2009.

681 Williams, J. T., Post, D. M., Cwyner, L. C., Lotter, A. F., and Levesque, A. J.: Rapid and
682 widespread vegetation responses to past climate change in the North Atlantic region,
683 *Geology*, 11, 971–974, 2002.

684 Witt, A. and Schumann, A. Y.: Holocene climate variability on millennial scales recorded in
685 Greenland ice cores, *Nonlinear Process. Geophys.*, 12, 345–352, 2005.

686 Yll, E.I., Perez-Obiol, R., Pantaleon-Cano, J., and Roure, J.M.: Palynological Evidence for
687 Climatic Change and Human Activity during the Holocene on Minorca (Balearic Islands),
688 *Quat. Res.*, 48, 339–347, 1997.

Depth (cm)	Material dated	¹⁴ C age yr BP	95,4 % (2σ) cal age ranges (BP)	Relative area under probability distribution	Median probability cal BP
60	Bulk	2535 ± 30	2494 – 2746	0,447	2624
120	Bulk	3220 ± 35	3371 – 3509	0,936	3436
170	Bulk	4390 ± 35	4859 – 5047	0,991	4949
240	Bulk	5200 ± 40	5897 – 6021	0,943	5958

Pollen taxa	Plant species
<i>Alisma</i>	<i>Alisma plantago-aquatica</i>
<i>Alnus</i>	<i>Alnus glutinosa</i>
<i>Berberis</i>	<i>Berberis hispanica</i>
<i>Brassica</i>	<i>Brassica</i>
<i>Campanula</i>	<i>Campanula afra</i>
Caryophyllaceae	Caryophyllaceae
<i>Centaurea</i>	<i>Centaurea cyanus</i>
Chenopodiaceae	Chenopodiaceae
Asteroidae	Compositae Subfam. Asteroidae
Cichorioideae	Compositae Subfam. Cichorioideae
<i>Corylus</i>	<i>Corylus avellana</i>
Cupressaceae	Cupressaceae
<i>Ephedra</i>	<i>Ephedra fragilis</i>
<i>Euphorbia</i>	<i>Euphorbia characias</i>
<i>Geranium</i>	<i>Geranium macrorrhizum</i>
<i>Helianthemum</i>	<i>Helianthemum canariense</i>
<i>Ilex</i>	<i>Ilex aquifolium</i>
<i>Juglans</i>	<i>Juglans regia</i>
<i>Myriophyllum</i>	<i>Myriophyllum aquaticum</i>
<i>Plantago</i>	<i>Plantago lanceolata</i>
Polygonaceae	Polygonaceae
Ranunculaceae	Ranunculaceae
<i>Salix</i>	<i>Salix pedicellata</i>
<i>Saxifraga</i>	<i>Saxifraga</i>
<i>Taxus</i>	<i>Taxus baccata</i>
<i>Urtica</i>	<i>Urtica dioica</i>
Papaveraceae	Papaveraceae
<i>Pinus</i>	<i>Pinus halepensis</i>
<i>Olea</i>	<i>Olea europaea</i>
<i>Paronychia</i>	<i>Paronychia argentea</i>
<i>Erica</i>	<i>Erica arborea</i>
<i>Quercus</i>	<i>Quercus ilex</i>
<i>Cedrus</i>	<i>Cedrus atlantica</i>
<i>Artemisia</i>	<i>Artemisia herba-alba</i>

691
692

Zones	Depth (cm)	Age (cal BP)	Pollen data description		
Zone I	250 – 190	6227 – 5171	AP	27 – 60%	- Mainly <i>Quercus</i> and <i>Olea</i> . - Peak of <i>Pinus</i> (47%) at 6100 cal BP then decreasing. - Low percentages of <i>Cedrus atlantica</i> with initial spread around 5800 cal BP.
			NAP	39 – 72 %	- Herbs dominated by Poaceae (11 – 48 %), <i>Illecebrum</i> (3 – 19 %), Apiaceae (2 – 5 %), Brassicaceae (1 – 5 %), Asteraceae (0 – 5 %), Cichorioideae (1 – 6 %), Chenopodiaceae (0.5 – 2 %) and Cereals (0 – 1 %).
			DT	18 – 26	- Rapid fluctuations
Zone II	190 – 111	5171 – 3651	AP	28 – 56 %	- <i>Pinus</i> dominates the pollen record but regresses at 5500 cal BP (from 44 to less than 2 %). - <i>Cedrus atlantica</i> continues to expand (0 – 5 %). - We observe a peak of Rosaceae (6 %).
			NAP	43 – 72 %	- Herbs are dominated by Poaceae, <i>Illecebrum</i> and Asteraceae which reach their maximum (53, 20 and 10 %, respectively). - Cereals disappear.
			DT	19 – 29	- Moderate to high with two peaks.
Zone III	111 – 60	3651 – 2351	AP	23 – 58 %	- Strong expansion of <i>Cedrus atlantica</i> and <i>Quercus</i> . - An abrupt decline of <i>Cedrus atlantica</i> around 2653 cal BP is recorded. - <i>Pinus</i> regresses as well but shows a peak of 20% at 3300 cal BP.
			NAP	41 – 76 %	- Herbs dominate the pollen record. - Sharp decline in Poaceae, Asteraceae, Chenopodiaceae and Caryophyllaceae at 5600 cal BP. - Appearance of Cereals around 2653 cal BP.
			DT	20 – 31	- High.
Zone IV	60 – 5	2351 – 173	AP	23 – 43 %	- Abundance of <i>Cedrus atlantica</i> , <i>Quercus</i> , <i>Olea</i> and Rosaceae. - Sharp decline and disappearance of <i>Pinus</i> .
			NAP	56 – 76 %	- Herbs continue to dominate the pollen record with Poaceae, Cereals, Brassicaceae, Chenopodiaceae and Caryophyllaceae which are most abundant. - Asteraceae, <i>Illecebrum</i> and Apiaceae decline. - Centaurea and Cichorioideae disappear.
			DT	21 – 32	- High.

693
694

695 **Table 1.** Radiocarbon ages for the Hach-I core. Calibrations were performed using Calib 7.1
696 (Stuiver and Reimer, 1986).

697 **Table 2.** Pollen taxa assigned to the most probable plant species in our plant database.

698 **Table 3.** Pollen zones identified in the fossil record using a constrained cluster analysis. AP:
699 arboreal pollen taxa, NAP: non-arboreal pollen taxa, DT: taxa diversity.

700 **Figure 1.** The study area. (a) Geographical location of the tabular and pleated Middle Atlas
701 (MA); (b) sketch of the geological and geomorphological characteristics of the Hachlaf area
702 (from Martin, 1973); (c) phytoecological map showing the main ecosystems and the location
703 of the Hachlaf Lake (Dayet Hachlaf) within an oak forest (from Lecompte, 1969).

704 **Figure 2.** (a) Lithology of the core Hach-I and radiocarbon ^{14}C dates; (b) age/depth model
705 from BACON software (Blaauw and Christen, 2011).

706 **Figure 3.** Diagram showing the sediment fractions (clay, silt and Sand/Silt ratio), the pollen
707 percentages of *Cedrus atlantica* and *Pinus*, geochemical elements ($\delta^{13}\text{C}$ [$\delta^{13}\text{C}\text{‰}$],
708 nitrogen to carbon ratio [C/N], total organic carbon [TOC], Total Nitrogen [NT]) and
709 carbonates concentrations (CaCO_3), January mean temperature (Tjan), Annual precipitation
710 (Pann), winter and summer precipitations (Pw and Ps) and precipitation seasonality index
711 (SI). The red rectangles are pointing the values of present-day Tjan, Pann, Pw and Ps
712 (HCEFLCD, 2004), the red line shows the limit 3.7 ka cal BP and the blue rectangle shows
713 the time interval of the cold phase 5.2 cal PB.

714 **Figure 4.** Density plots of Tjan for the three dominating *Quercus* species in Morocco (*Q. ilex*,
715 *Q. coccifera* and *Q. suber*). The median values are the following for *Q. ilex*: 6.5°C, *Q.*
716 *coccifera* = 7.4°C and *Q. suber* = 7°C.

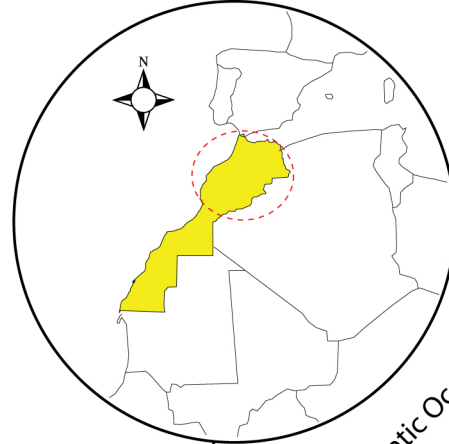
717 **Figure 5.** Diagram showing the percentages of the main pollen taxa identified in the Hach-I
718 core. Cyperaceae and Juncaceae are included within aquatic taxa. The dashed black curves
719 shows an exaggeration ($\times 7$) of the percentages of some taxa. On the right, pollen zones with their
720 boundaries are set up using a constrained hierarchical clustering (R Development Core Team, 2013).
721 The taxonomic diversity is computed using a rarefaction analysis. The red line shows the limit 3.7 ka
722 cal BP.

723 **Figure 6.** $\delta^{13}\text{C}$ and C/N bi-plot (from Meyers, 1994).

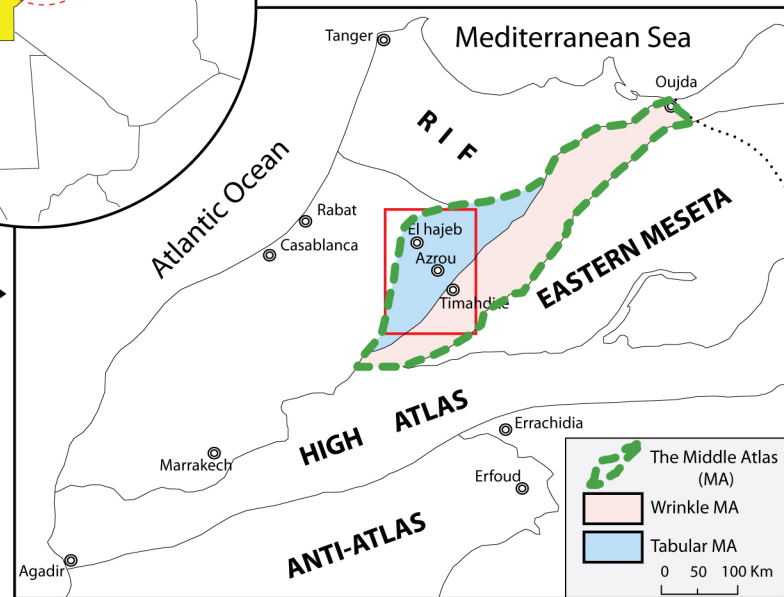
724 **Figure 7.** Pairwise correlation between the three climatic variables (Tjan, Pann and SI) and
725 the chemical elements.

726 **Figure 8.** Modern SI (upper panel) and Pann (middle panel) from the gridded WorldClim
727 dataset (Hijmans et al., 2005) over Morocco. The lower panel shows the distribution of Pann
728 vs. SI: the lowest index occurs in southern Morocco where Pann is lower than 200 $\text{mm}\cdot\text{y}^{-1}$
729 and the highest index occurs in the high altitudinal areas (Middle Atlas and Rif mountains).

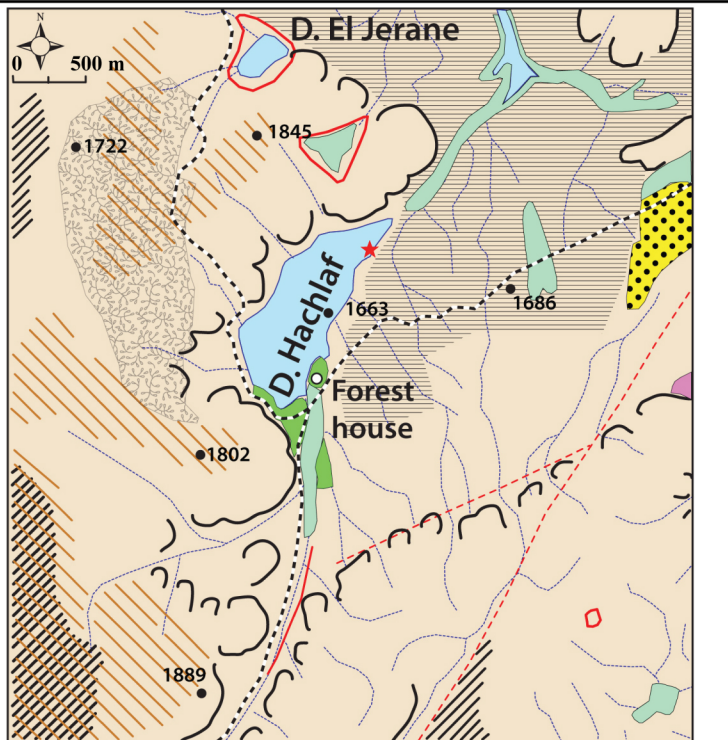
730



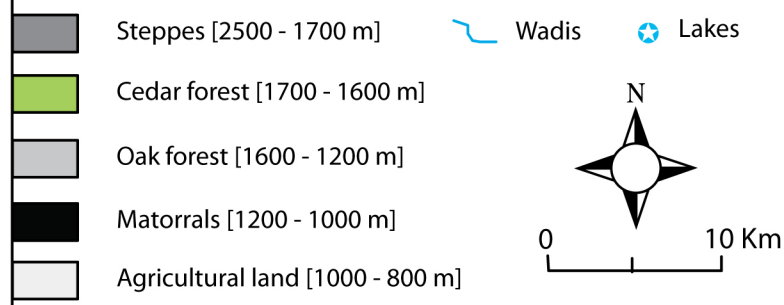
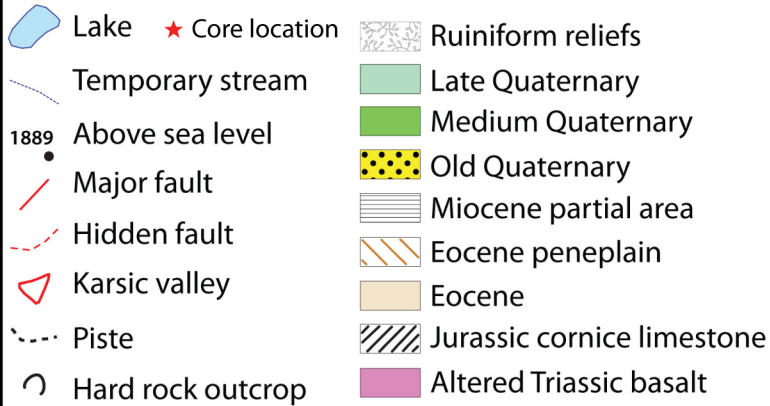
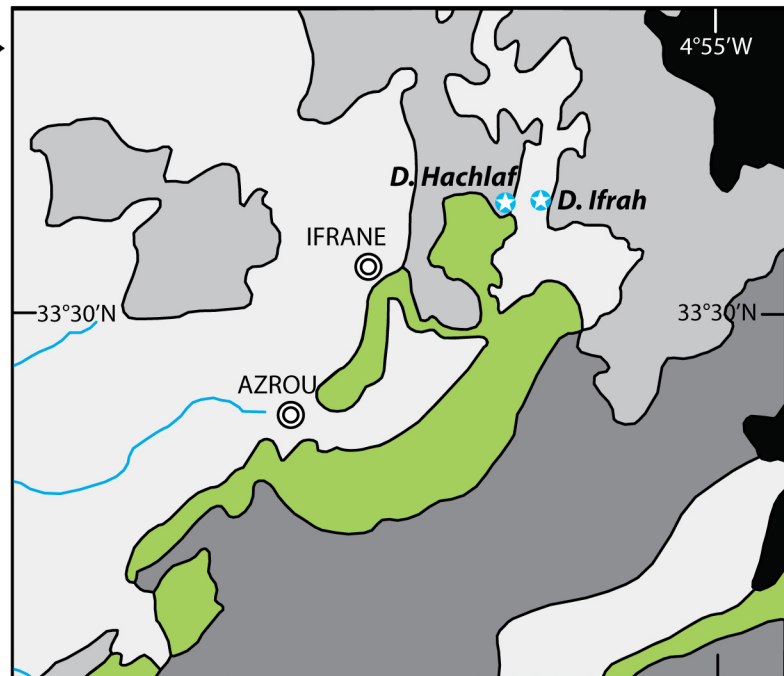
a

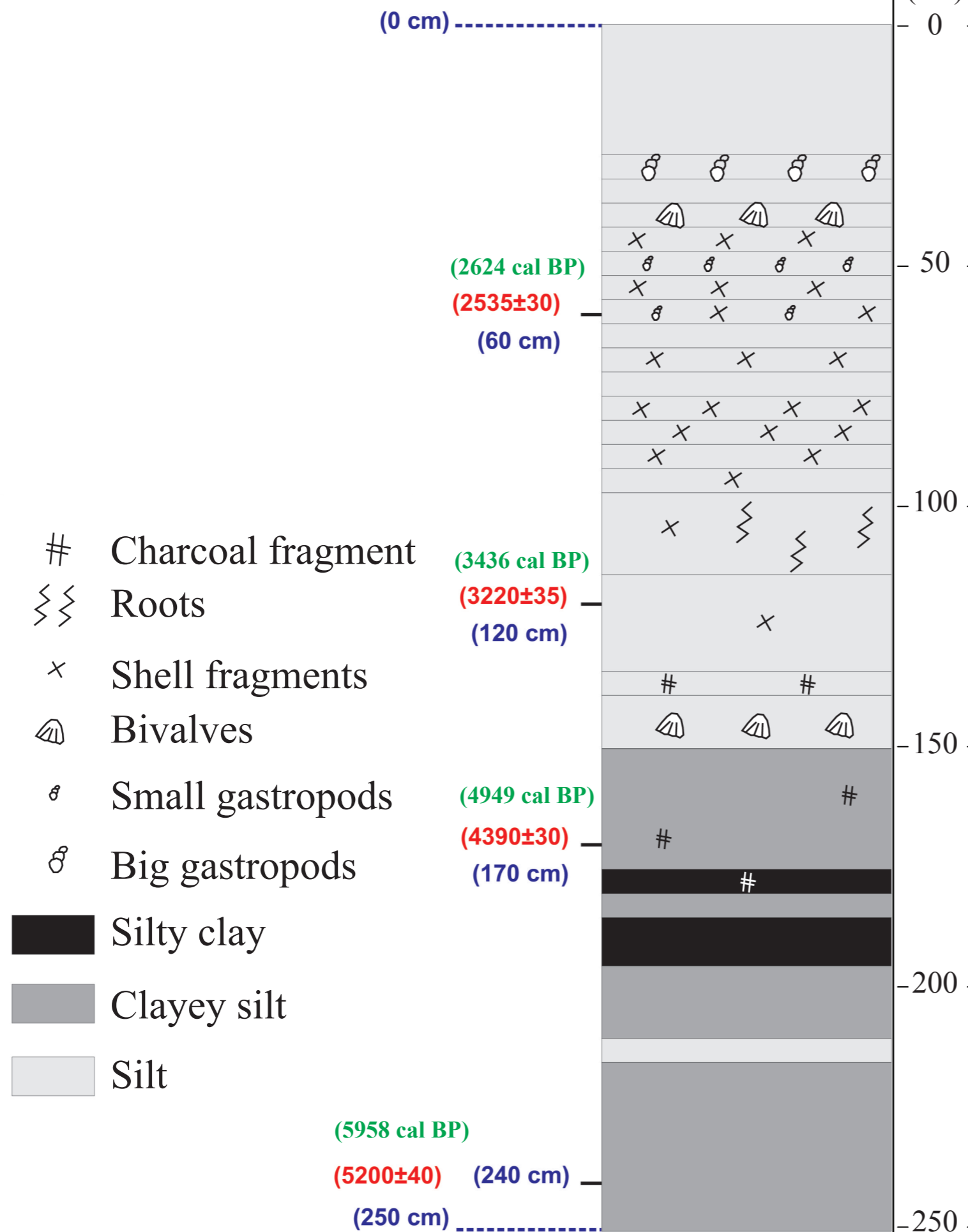
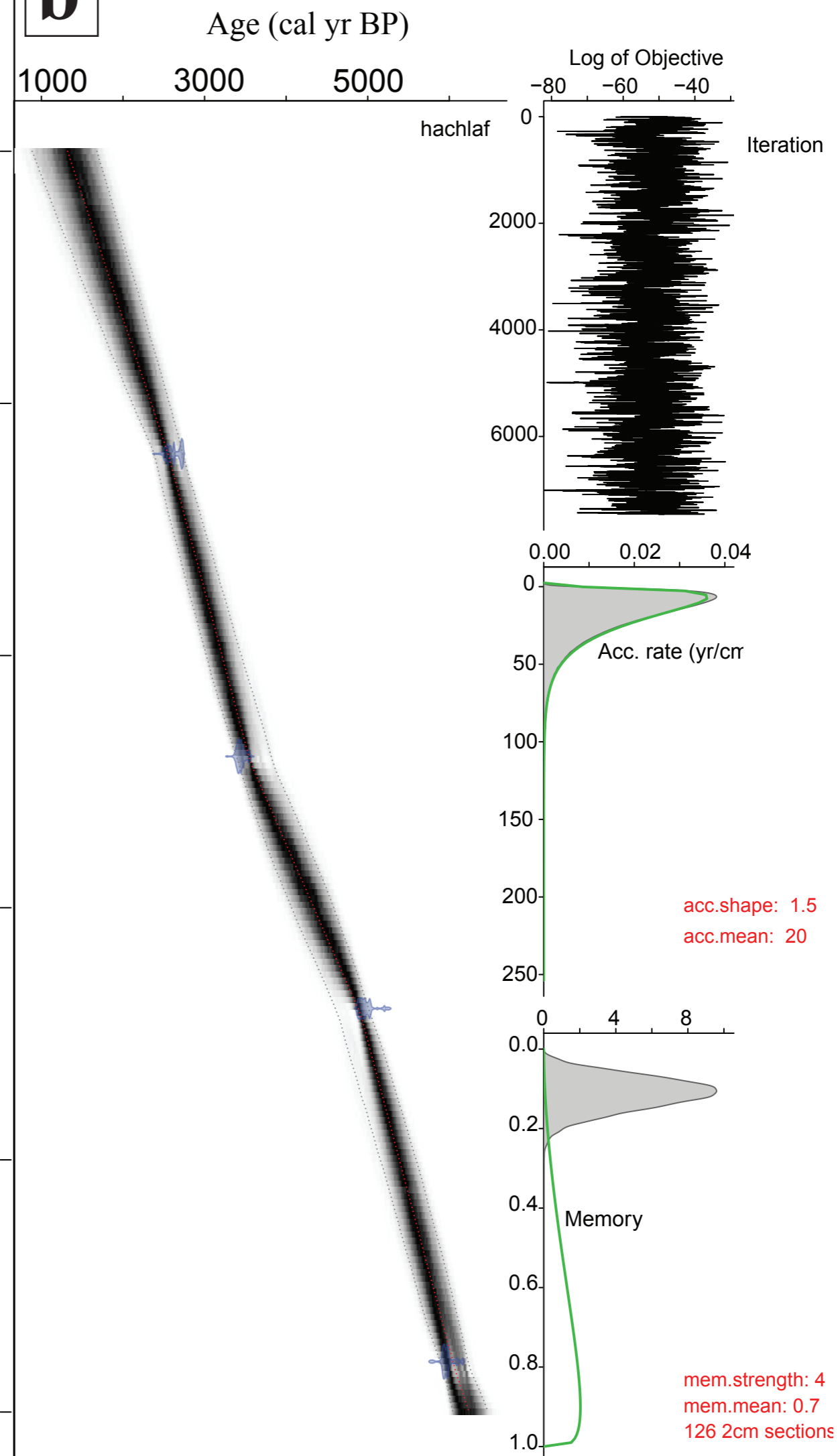


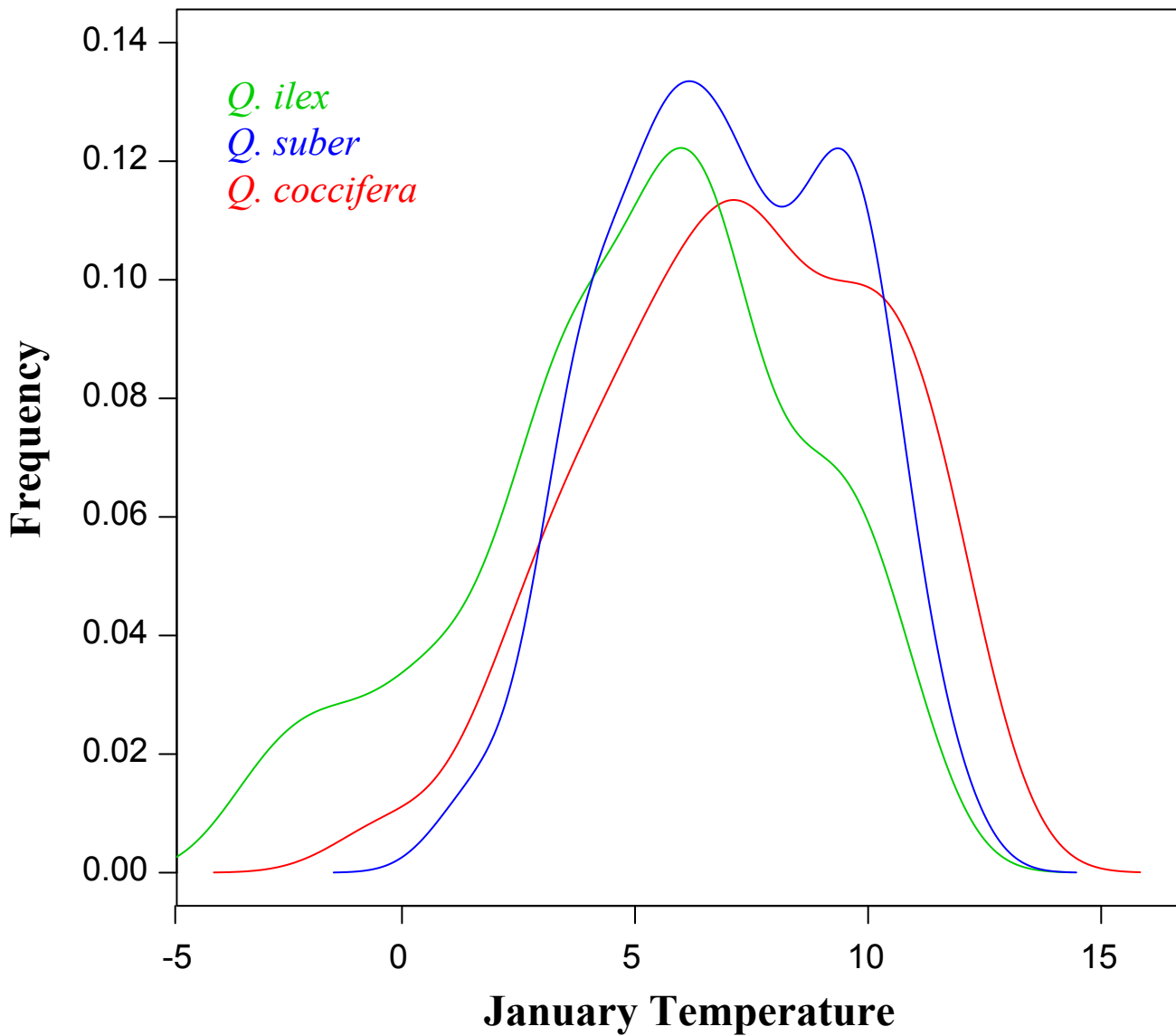
b

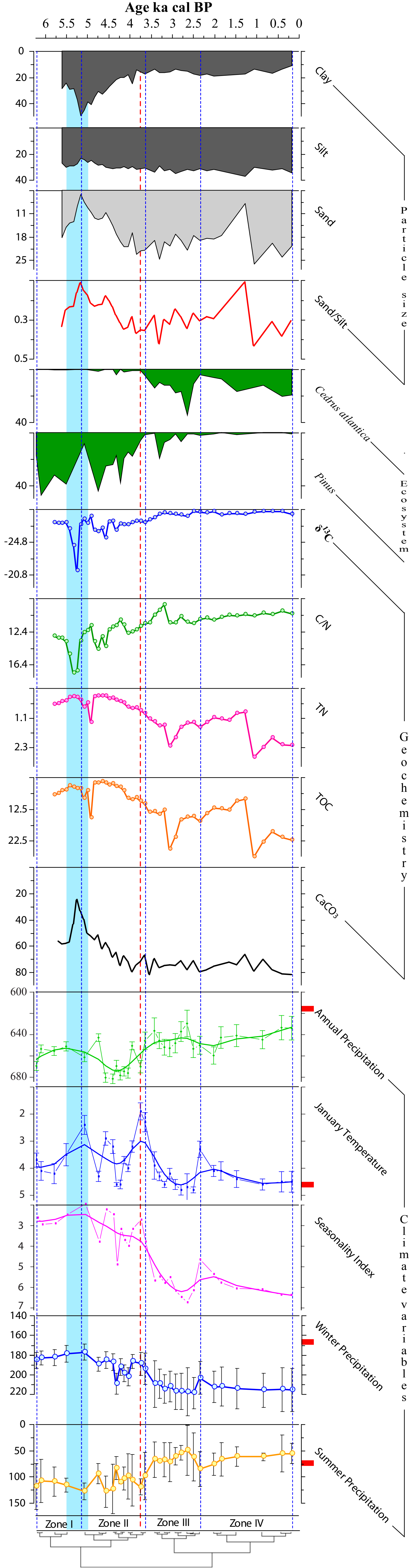


c



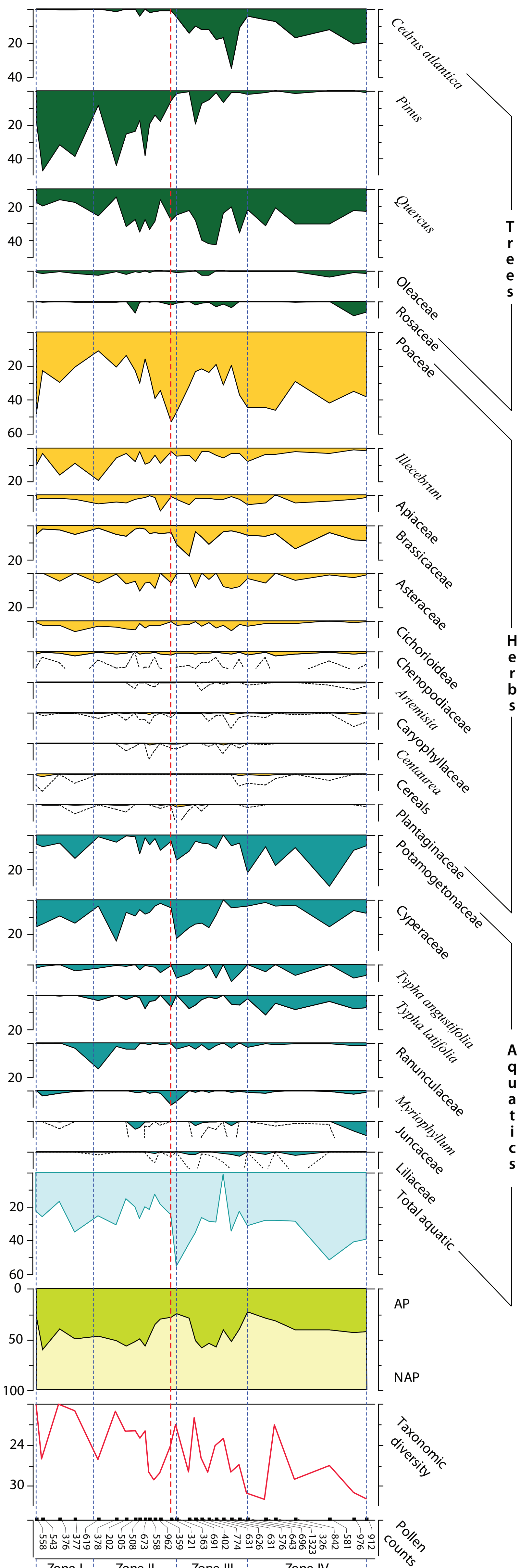
a**b**





Age ka cal BP

6 5.5 5 4.5 4 3.5 3 2.5 2 1.5 1 0.5 0



C3 metabolism plants

